Short Communication

Effect of MXene on Oxygen Ion Conductivity of $Sm_{0.2}Ce_{0.8}O_{1.9}$ as Electrolyte for Low Temperature SOFC

Hongxi Xian[1,2], Chanchan Fan[1], Peng Zhang[1], Ranran Wang[1], Chenxi Xu[1,*], Hua Zhai[2,3,*], Tao Hong[1], Jigui Cheng

[1] School of Materials Science and Engineering, Hefei University of Technology, Hefei, Anhui, China, 230009
[2] Institute of Industry & Equipment Technology, Hefei University of Technology, Hefei, Anhui, China, 230009
[3] Key Lab of Aerospace Structural Parts Forming Technology and Equipment of Anhui Province, Hefei University of Technology, Hefei, China, 230009
[*]E-mail: xuchenxi31@126.com, jxzhaihuajx@hfut.edu.cn

Low temperature solid oxide fuel cell (SOFC) has received great interest recently. However, the low oxygen ion conductivity of electrolyte restricts the operation temperature reduction for SOFC. In this report, 2D nanomaterial $Ti_3C_2T_x$ is used as filler doped into the $Sm_{0.2}Ce_{0.8}O_{1.9}$（SDC）to enhance the conductivity and mechanical strength of composite electrolyte. The 5wt.% $Ti_3C_2T_x$/SDC composite membrane exhibits the 3 and 9 times ionic conductivity as that of SDC at 500°C and 600°C, respectively. Furthermore, the peak power density of the single cell enhanced by ∼250% at 500°C. The addition of $Ti_3C_2T_x$-MXene also improved the hardness, fracture toughness and thermal stability of composite membranes.

Keywords: MXene, composite electrolyte, low temperature SOFC, Mechanical Strength

1. INTRODUCTION

Solid oxide fuel cells (SOFC) have attracted much attention because of their safety, low cost and long life operation period [1, 2]. The key issue limits the development of SOFC commercialized application is the high operating temperature that resulting in a high systems costs, fast performance degradation rates, and long-time start-up. Therefore, SOFC worked below 600°C is the promising way to reduce costs and commercial development.

As the key part of SOFC, The electrolyte material should have high oxygen ion conductivity and good mechanical strength at low temperature (≤600°C). The electrolyte should have high compactness

and mechanical strength that is convenient for processing. In addition，the good chemical compatibility and thermal matching with the electrode material are also required. The oxygen ion conductivity decreases with the temperature dropping, so the electrolyte material with high conductivity at low temperature is the main challenge [2, 3]. The doped CeO_2-based electrolyte which mainly includes Sm^{3+} doped SDC and Gd^{3+} doped GDC is the widely used electrolyte material for medium temperature (600-800°C) SOFC. The thinner electrolyte normally provides high conductivity because of the short oxygen ion transfer path. However, the strength of membrane would become the other issue that limit the lifetime [4-6]. So, the conductivity of membrane could be improved by increasing the strength at low temperature (400-600°C).

Recently, 2D nanomaterials MXenes have attracted great attention because of their good conductivity and mechanical strength [7-11]. MXene is normally obtained by selectively etching A elements from the MAX phase [12, 13]. The MAX phase whose chemical formula is generally described as $M_{n+1}AX_n$ (n=1, 2 or 3, M represents a class of transition metal, A represents the third or fourth main group elements, and X is carbon or nitrogen atom). The surfaces of MXene contains hydroxyl, oxygen and fluoride groups which could provide long-range protons or ions transfer pathways in the matrix [14, 15]. Fei reported the proton conductivity improved by $\sim$200% with the incorporation of 3wt% $Ti_3C_2T_x$-MXene into PBI membranes [16]. However, the influence of MXene to oxygen ion conductivity and mechanical strength in the SDC is still not clear.

In this work, $Ti_3C_2T_x$ was chosen as MXene. 5wt% $Ti_3C_2T_x$-MXene was used into SDC electrolytes to enhance the oxygen ion conductivity for low temperature SOFCs. $Ti_3C_2T_x$ can enhance the thermal stability, hardness and fracture toughness of electrolyte membranes. The single cell performance test showed that the peak power density was enhanced at 500°C.

2. EXPERIMENTAL

2.1 Preparation of $Ti_3C_2T_x$/SDC composite membranes

SDC was prepared as reported [17]. Briefly, a 0.2 mol $Sm(NO_3)_3 \cdot 6H_2O$: 0.8 mol $Ce(NO_3)_3 \cdot 6H_2O$ was mixed in de-ionized water, and then 0.4 mol $C_2H_5NO_2$ was added into the mixed solution. The mixed solution was stirred continuously in a ceramic pan at 250°C until a thick slurry was obtained. The oxide powder was kept at 700°C for 2 hours to remove organic solvent. $Ti_3C_2T_x$ stand for MXene (T represent the surface group such as –OH, -F etc.) was obtained by etching the Al atom layer from Ti_3AlC_2 (MAX) by HF [18]. 5wt.% $Ti_3C_2T_x$ was mixed with SDC in the ethanol. The mixed solution was dried at 60°C for 5 hours. The 5wt.% $Ti_3C_2T_x$/SDC composite powders were pressed under a pressure of 250 MPa, and it was sintered for 5 h at 1450 °C in the oven.

2.2. Characterizations

The morphologies of the 5wt.%$Ti_3C_2T_x$/SDC composite membranes were investigated via a SU-8020 Scanning Electron Microscope. The crystal structures were analyzed from 5–90° by X-ray diffraction (XRD, X'Pert PROMPD). The Thermal stability from 20 to 600°C was analyzed by thermos-

gravimetric analysis (TGA, STA449F3). The mechanical behavior was analyzed by HV-5 type digital display Vickers hardness instrument. The fracture toughness of SDC and 5wt.%Ti$_3$C$_2$T$_x$/SDC membrane composite electrolyte samples was investigated by indentation method (Eq. (1)), which is calculated by the following equation [19, 20].

$$K_{IC} = 0.203*HV*a^2*c^{-1.5}, \qquad\qquad\qquad (1)$$

where K_{IC} is fracture toughness, MPa $*m^{1/2}$; Hv is Vickers hardness, GPa; a is an average length of the indentation diagonal, μm; c is a half of crack length, μm.

The ionic conductivity was carried out at a perturbation voltage of 0.20V and a frequency range of 10 Hz to 10^6 Hz. The test temperature were carried out at the range of 400 to 600°C. The electrochemical performance of the composite membranes was tested by AutolabPGSTAT302 with the cathode materials are Ni as the anode and BaCo$_{0.4}$Fe$_{0.4}$Zr$_{0.1}$Y$_{0.1}$O$_3$[21] as the cathode, respectively.

3. RESULTS AND DISCUSSION

XRD patterns of Ti$_3$AlC$_2$, Ti$_3$C$_2$T$_x$, SDC and 5wt.% Ti$_3$C$_2$T$_x$/SDC powders are exhibited in Fig.1. (111), (200), (220), (311), (222), (400), (331), and (420) crystal planes are corresponding to the angles at 28.516°, 33.059°, 47.371°, 56.169°, 69.325°, 76.416°,78.832°, and 88.129° of SDC which is consistent with the diffraction peaks of the SDC reported in the literature[17]. The diffraction peak (001) of Ti$_3$C$_2$T$_x$ left shifts to around 6° from 10.2° of Ti$_3$AlC$_2$ that the distance of the layer becomes 5.68 nm [18]. This indicates Ti$_3$C$_2$T$_x$ successfully etched from the Ti$_3$AlC$_2$ phase. The 002 peak of SDC can be also clearly seen in the 5wt.%Ti$_3$C$_2$T$_x$/SDC composite powder at 6°, which evidenced that Ti$_3$C$_2$T$_x$ is successfully doped in SDC powder.
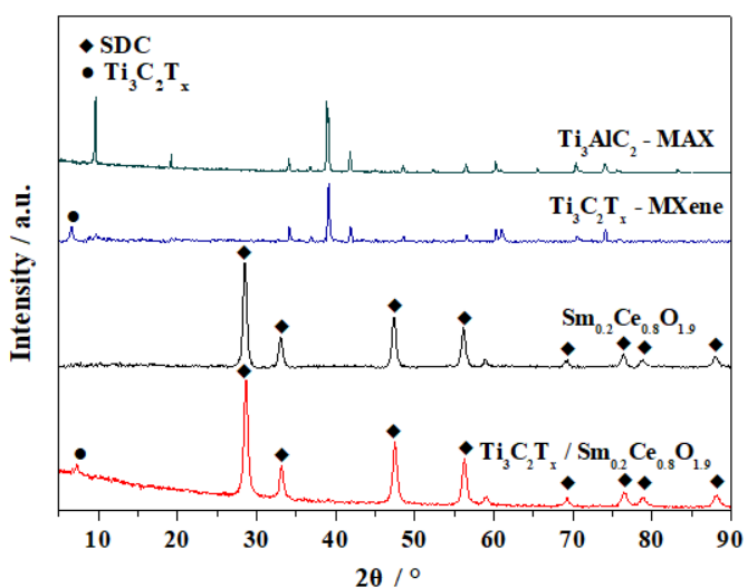
Figure 1. XRD patterns of Ti$_3$AlC$_2$, Ti$_3$C$_2$T$_x$, SDC and 5wt.%Ti$_3$C$_2$T$_x$/SDC

The microscopic morphologies of SDC and 5wt.% Ti$_3$C$_2$T$_x$/SDC electrolyte membranes are depicted in Fig.2. It is observed that the SDC and Ti$_3$C$_2$T$_x$/SDC membrane is completely dense. Fig 2(b)

shows the $Ti_3C_2T_x$-MXene particles are evenly dispersed inside the SDC matrix. There are no obvious pores were found in the composite membranes indicating the more compactness of electrolyte. The micro structure of the composite membrane is clearly visible and compactness. There are no visible defects observed in $Ti_3C_2T_x$/SDC which could inhibit the gas crossovers. The lamellar structure of $Ti_3C_2T_x$ in the composite membranes is beneficial to the formation of oxygen ion path way which can enhance the ionic conductivity [17].

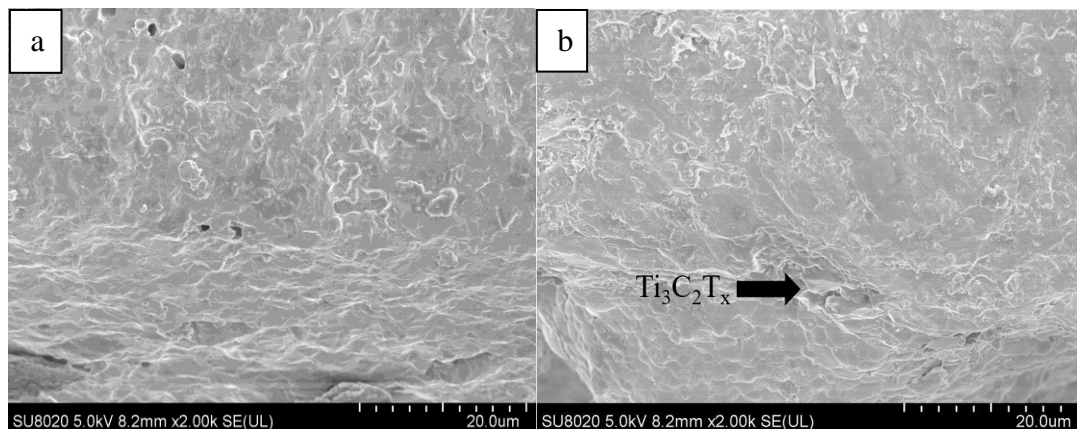**Figure 2.** SEM images of membrane cross-sections: a) SDC, b) 5wt.% $Ti_3C_2T_x$/SDC

The thermal stability of SDC and 5wt.% $Ti_3C_2T_x$/SDC membranes are studied from 25 to 600°C depicted in Fig.3. The mass loss of SDC and $Ti_3C_2T_x$/SDC are 6% and 4%, respectively. The thermal curves of SDC based materials are stability for the high temperature stability that ensure the membrane could be operation at the work condition. Furthermore, the composite powder shows better thermal stability than pristine SDC powder, which indicating the MXene could further enhance the stability of materials.
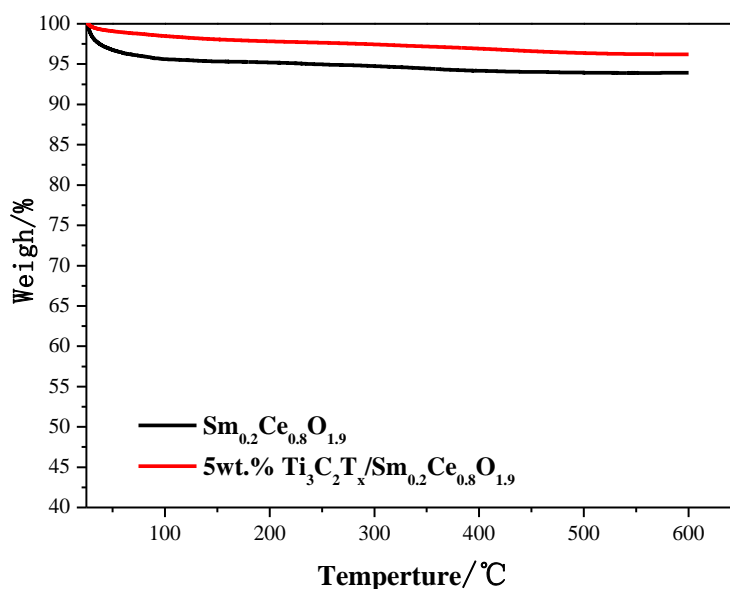

Figure 3. TGA of the SDC and 5wt.% $Ti_3C_2T_x$/SDC from room temperature to 600 °C

The hardness HV of two samples were exhibited in table 1. The HV of SDC sample is 0.085GPa under the load of 9.07N for 10 seconds. The hardness of composite membrane sample reaches 0.101GPa. The indentations and cracks of the SDC and $Ti_3C_2T_x$/SDC membranes are observed in Fig.4. The fracture toughness of SDC and $Ti_3C_2T_x$/SDC membrane are 7.86 MPa·um$^{1/2}$ and 31.77 MPa·um$^{1/2.}$ as shown in table 1, respectively. The toughness of 5wt.% $Ti_3C_2T_x$/SDC is 4 times of that of pristine SDC. The composite membrane is more compact with higher hardness and toughness. The increase in the hardness and fracture toughness may be attributed to the following reasons. 1) $Ti_3C_2T_x$ located at the interface of SDC grains by growing firmly during the high-temperature sintering process that could deflect the growth of micro-cracks. It results in the stress release and the hardness and toughness increasing; 2) $Ti_3C_2T_x$ anchored at the grain boundary could enhance the interfacial friction between the SDC [19-21].

Table 1. Hardness and fracture toughness of SDC and 5 wt.% $Ti_3C_2T_x$/SDC membrane

Experimental Materials	Load (N)	Time (s)	Hardness (GPa)	Fracture toughness (MPa um$^{1/2}$)
$Sm_{0.2}Ce_{0.8}O_{1.9}$	9.807	10	0.085	7.86
$Ti_3C_2T_x$/$Sm_{0.2}Ce_{0.8}O_{1.9}$	9.807	10	0.101	31.77

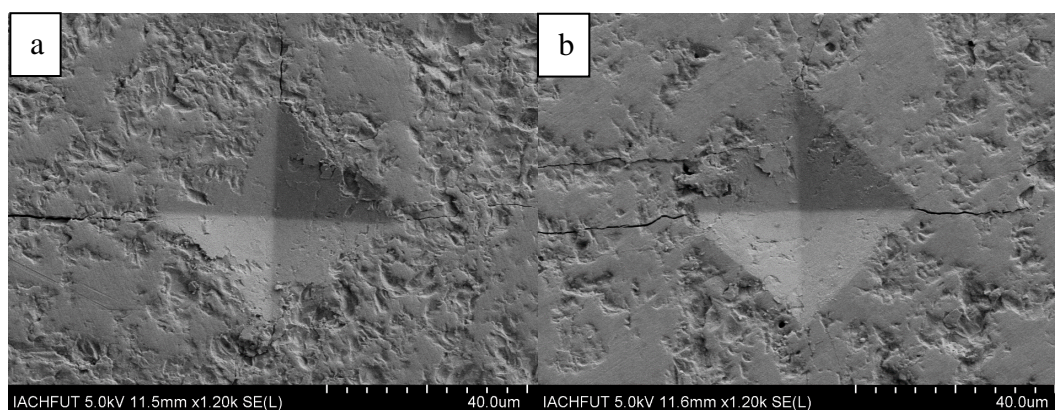**Figure 4.** SEM images of the indentations and cracks: a) SDC, b) 5wt.% $Ti_3C_2T_x$/SDC

The conductivities of the SDC and 5wt.%$Ti_3C_2T_x$/SDC membranes are depicted in fig. 5. The conductivity of the SDC increases from 1.12×10^{-3} S cm^{-1} to 1.35×10^{-2} S cm^{-1} among the temperature range of 450°C to 600°C. The conductivity of the $Ti_3C_2T_x$/SDC increases from 2.43×10^{-3} S cm^{-1} to 1.26×10^{-1} S cm^{-1} in the range of 450-600°C. The conductivity of 5wt.%$Ti_3C_2T_x$/SDC composite membrane is obviously higher than that of pristine SDC. The oxygen ionic conductivities of SDC are around 1.0×10^{-2} S cm^{-1} at 600° in the literature [22,23]. At the similar temperature, the conductivity of the $Ti_3C_2T_x$/SDC composite membrane is 9-fold improvement. These may be associated with $Ti_3C_2T_x$ particles provide more jumpable sites and transmit path for oxygen ion.

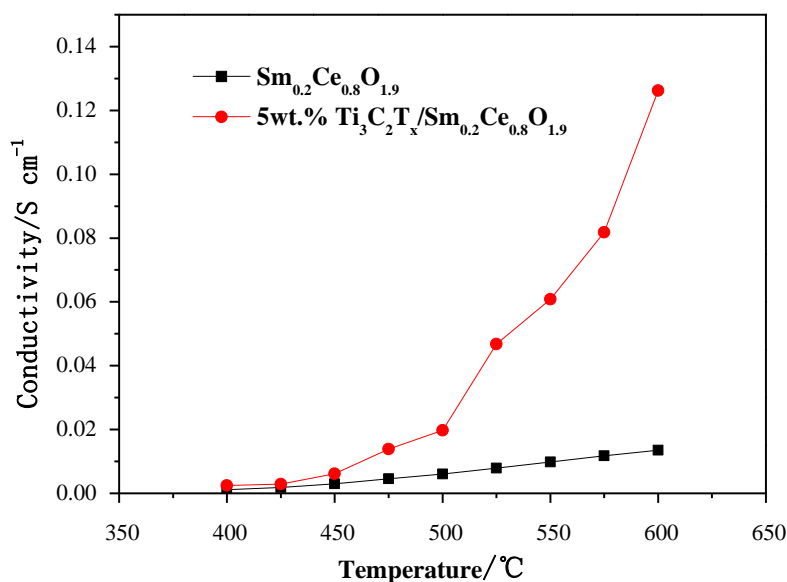**Figure 5**. The conductivities of SDC and 5wt.% $Ti_3C_2T_x$/SDC membranes

The comparison $Ti_3C_2T_x$/SDC composite membrane and electrolytes normally used for SOFC in literatures are exhibited in Table 2. The conductivity of SDC is normally less than 0.1 S cm^{-1} at low temperature according to the literature and our result [28]. The conductivity of $Ti_3C_2T_x$/SDC exhibits the best conductivity which is even orders of magnitude higher than that of reported membranes. Therefore, the $Ti_3C_2T_x$/SDC pellet as the electrolyte membranes provide a competitive conductivity at lower operating temperatures of 600°C which could be considered as potential materials for low temperature SOFC. In conclusion, incorporating moderate ion conductor into membrane is an effective method to improve the electrolyte's conductivity.

Table 2. Comparison the conductivity of membranes

Membrane	Ionic conductivity (S cm^{-1})	Ref
CeO_2	1×10^{-5} at 600°C	24
YSZ	2.12×10^{-2} at 800°C	25
SDZ	1×10^{-1} at 800°C	26
Bi_2O_3	1×10^{-1} at 800°C	27
SDC	$8*10^{-2}$ at 550°C	28
SDC	1.35×10^{-2} at 600°C	This paper
5 wt.% $Ti_3C_2T_x$/SDC	1.26×10^{-1} at 600°C	This paper

Fig. 6 demonstrates fuel cell performance based on SDC and 5 wt.% $Ti_3C_2T_x$/SDC membranes under H$_2$/air at 500°C, respectively. At 500 °C, the open circuit voltages of the 5 wt.% $Ti_3C_2T_x$/SDC membranes are 0.82 V which is 0.08 V higher than that of SDC indicating composite membrane exhibits less crossover. The peak power density of SDC membrane and 5 wt.% $Ti_3C_2T_x$/SDC composite

membrane are 0.96 mW cm^{-2} and 2.42 mW cm^{-2}, respectively. The performance of Ti$_3$C$_2$T$_x$/SDC exhibits 1.5-fold improvement comparing to that of the SDC membrane at 500°C. The addition of Ti$_3$C$_2$T$_x$ particles provide more transport channels for oxygen ion conduction which is consistent with the conductivity results. However, the performance is still high enough at low temperature that electrode materials and MEA technology should be further optimized for low temperature SOFC.
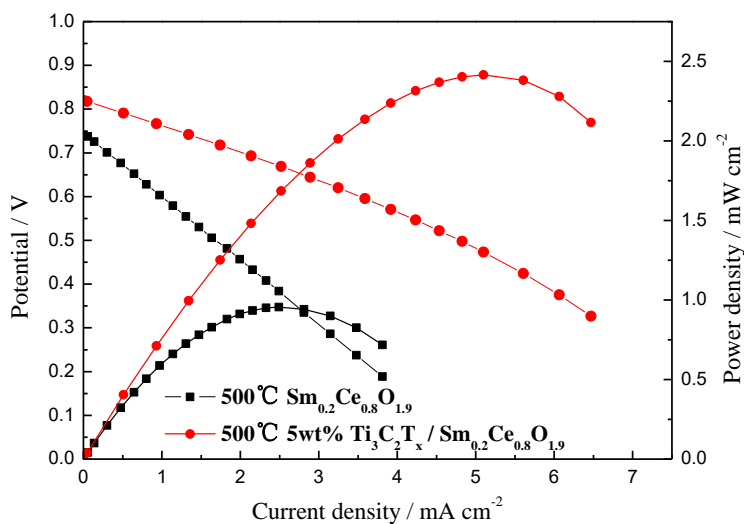

Figure 6. Polarization and power density curves of SDC and 5wt.% Ti$_3$C$_2$T$_x$/SDC membranes operated with H$_2$/O$_2$ atmospheric pressure at 500°C.

4. CONCLUSIONS

In this study, Ti$_3$C$_2$T$_x$ particles fills are doing in the interfacial of SDC grains and improves the compactness of the electrolyte membrane. The addition of 5wt% Ti$_3$C$_2$T$_x$ improved the fracture toughness, conductivity and electrochemical performance by ~400%, ~900%, ~250%, respectively. The maximum power densities of SDC and Ti$_3$C$_2$T$_x$/SDC electrolyte membranes were 0.956mW cm^{-2} and 2.415mW cm^{-2}, respectively. These results pointed out that Ti$_3$C$_2$T$_x$ standing for MXene could be a feasible additive for improving the performance of SDC electrolyte membranes for low temperature SOFC.

References

1. B. Zhu, X.R. Liu, Z.G. Zhu, R. Ljungberg, *Int. J. Hydrogen. Energy.*, 33 (2008) 3385.
2. S.P.S Badwal, F.T. Ciacchi, D. Milosevic, *Solid State Ion.*, 136 (2000) 91.
3. X.F. Guan, H.P. Zhou, Y. Wang, J. Zhang, *J. Alloy. Compd.*, 464 (2008) 310.

4. T.J. Huang, J.F. Li, *J. Power Sources*, 181 (2008) 62.

5. M. Shi, N. Liu, Y.D. Xu, C. Wang, Y.R. Yuan, P. Majewski, F. Aldinger, *J. Mater. Process. Tech.*, 169 (2005) 179.

6. C. A. Tian, D. Biao, Y.W. Zeng, *J. Mater. Sci*, 24 (2006) 627.

7. Y.H. Liu, J.T. Wang, H.Q. Zhang, C.M. Ma, J.D. Liu, S.K. Cao, X. Zhang, *J. Power Sources*, 269 (2014) 898.

8. Z.W. Hu, G.H. He, S. Gu, Y.F. Liu, X.M. Wu, *J. Appl. Polym. Sci.*, 131 (2014) 1082.

9. N. Uregen, K. Pehlivanoglu, Y. Ozdemir, Y. Devrim, *Int. J. Hydrogen. Energy.*, 42 (2017) 2636.

10. C.X. Xu, Y.C. Cao, R. Kumar, X. Wu, X. Wang, K. Scott, *J. Mater. Chem.*, 21 (2011) 11359.

11. C.X. Xu, X.T. Liu, J.G. Cheng, K. Scott, *J. Power Sources*, 274 (2015) 922.

12. M. Naguib, V.N. Mochalin, M.W. Barsoum, Y. Gogotsi, *Adv. Mater.*, 26 (2014) 992.

13. J. Halim, M.R. Lukatskaya, K.M. Cook, J. Lu, C.R. Smith, L.A. Naslund, S.J. May, L. Hultman, Y. Gogotsi, P. Eklund, M.W. Barsoum, *Chem. Mater.*, 26 (2014) 2374.

14. M. Ghidiu, M.R. Lukatskaya, M.Q. Zhao, Y. Gogotsi, M.W. Barsoum, *Nature*, 516 (2014) 78.

15. M.A. Hope, A.C. Forse, K.J. Griffith, M.R. Lukatskaya, M. Ghidiu, Y. Gogotsi, C.P. Grey, *Phys. Chem. Chem. Phys.*, 18 (2016) 5099.

16. Y. Xie, M. Naguib, V.N. Mochalin, M.W. Barsoum, Y. Gogotsi, X.Q. Yu, K.W. Nam, X.Q. Yang, A.I. Kolesnikov, P.R.C. Kent, *J. Am. Chem. Soc.*, 136 (2014) 6385.

17. N. Ai, Z. Lu, K.F. Chen, X.Q. Huang, B. Wei, Y.H. Zhang, S.Y. Li, X.S. Xin, X.Q. Sha, W.H. Su, *J. Power Sources*, 159 (2006) 637.

18. X. L. Zhang, C. C. Fan, N. Y. Yao, P. Zhang, T. Hong, C. X. Xu, J. G. Cheng, *J. Membr. Sci.*, 7388 (2018) 31433

19. X.L. Meng, C.H. Xu, G.C. Xiao, M.D. Yi, Y.B. Zhang, *Ceram. Int*, 42 (2016) 16090.

20. M. M. Fei, R. Z. Lin, Y.W. Lu, X. L. Zhang, R. J. Bian, J. G. Cheng, P. F. Luo, C. X. Xu, D.Y. Cai, *Ceram. Int.*, 43 (2017) 17506.

21. M. Shang, J. H. Tong, R. O'Hayre, *Rsc. Adv.*, 3 (2013) 15769.

22. H. B. Li, C. R. Xia, M. H. Zhu, Z. X. Zhou, G.Y. Meng. *Acta. Mater.*, 54 (2006) 721.

23. R. R.Peng, C. R. Xia, Q. X. Fu, G.Y. Meng, D. K. Peng, *Mater. Lett.*, 56 (2002) 1043.

24. R. P. Singh, R. Bhattacharyya, S. Omar, *Solid State Ion.*, 309 (2017) 1.

25. S. K. Vijay, V. Chandramouli, S. Khan, P. C. Clinsha, S. Anthonysamy, *Ceram. Int.*, 40 (2014), 16689.

26. T. S. Zhang, J. Ma, H. Cheng, S. H. Chan, *Mater. Res. Bull.*, 41 (2006), 563.

27. N.V. Skorodumova, A.K. Jonsson, M. Herranen, M. Stromme, G.A. Niklasson, B. Johansson, S.I. Simak, *Appl. Phys. Lett.*, 86 (2005) 1801.

28. Y. Meng, X. Wang, W. Zhang, C. Xia, Y. Liu, M. Yuan, B. Zhu, Y. Ji, *J. Power Sources*, 421(2019) 33